A Unified Constitutive Model for Creep-Plasticity Interaction with Microstructure

QIAN Zhengfang, FAN Jinghong
Chongqing University, Chongqing, China

1 INTRODUCTION

Constitutive modeling of inelastic behavior of materials at elevated temperature has made great progress during the past fifteen years, specially in developing of various unified rate(time) dependent constitutive models. However, one of the incompletely solved problems concerns creep-plasticity interaction which is very important in the design of reactor components in high temperature. Ohashi(1986) has reported some serious interaction effects between creep and plasticity for type 316 stainless steel at elevated temperature. Furthermore, joint-work on evaluation of ten kinds of inelastic constitutive models under creep-plasticity interaction for 2.25 Cr-1 Mo steel at 600℃ showed that both conventional models of superposition types and unified ones could not describe satisfactorily the experimental results(Inoue et al. 1986, 1987) . Actually, all unified constitutive models currently in effect can not predict that creep resistance is markedly greater than plasticity one(Ohashi et al. 1986). Also, very important dislocation substructure and its inhomogeneous internal stress distribution as well as its hardening effects are not taken into account in these models. In the other hand, recently proposed non-unified constitutive models(Fan et al. 1989; Contesti et al.1989)had a set of equations for creep and plasticity respectively. Apart from complexity and more material constants,there is artificial factor more or less in the rule of coupling between creep and plasticity. In practical applications, however, creep and plasticity are observed simultaneously or alternately. So, it is hard to separate creep and plasticity, specially under complex loading history.

An important progress in connecting phenomenological constitutive models with dislocation microstrutures was carried out (Eifantis, 1987). This continuum framwork with microstructure, however, is still at the structure of single slip systerm and appropriate modification is needful in the averaging procedure of the orientation tensor.

2 MICROMECHANISM OF CREEP-PLASTICITY INTERACTION

As pointed by Nix(1980), for pure metals and class II solid solutions the substructure plays a dominant role in creep. The information about formation and evolution of substructure provides strong guidelines for theoretical modeling of the creep process. An important feature of substructure is its heterogenety. A typical experimental measurement of dislocation density from Orlova(1973) is shown in fig.1. Such a evolution picture of dislocation substructures may occur repeatly and is of general significance. Correspondingly, heterogeneous

SMiRT 11 Transactions Vol. L (August 1991) Tokyo, Japan, © 1991

substructure causes the internal (dislocation) stresses in the solid to become nonuniform. Experimental measuring of local stress field for Al-Zn alloy(Martin, 1985)showed that local stresses near subgrain boundaries are several times larger than stresses within subgrains, and these decrese rapidly with the distance from it.

Power-law creep is the primary source of creep for most engineering components subjected to typical stress range σ/μ from $10^{-4}\sim10^{-2}$ and temperature above 0.5 Tm (Tm is the melting point of material), and two basic inelastic deformation mechanisms for a polycrystalline metal are dislocation glide and dislocation climb controlled both by thermal activiated process according to the study of deformation mechanisms(Frost et al. 1982). From above investigation about the formating process of dislocation substructure and its evolution of dislocation density as well as its heterogenety of internal stresses, we can conclude that the processes of dislocation glide-plus-climb are a control mechanism of creep-plasticity interaction effects. Such a simple picture of dislocation movements is shown is fig.2. Important interaction effect between glide and climb of dislocations is that local high stresses near subgrain boundaries caused by glide dislocation pileups relax markedly due to climb of dislocations, which affects both dynamic recovery and static thermal recovery and accomplishes in the manner of reaction-diffusion within an interface between subgrains and subgrain boundaries.

3 MACROSCOPIC REPRESENTATION OF ORIENTATION TENSOR

It should be noticed that inelastic strain is mainly produced by dislocation glide even if inelastic deformation process is directly(or indirecly) controlled by diffusion under creep-plasticity interaction conditions. The inelastic strain contributed by dislocation climb is relatively small and can be negligible. By definiting of geometry of dislocation glide, local inelastic strain rate tensor $\dot{\boldsymbol{\varepsilon}}^{s}$ in a grain or a subgrain is given by:

(1a) $\dot{\boldsymbol{\varepsilon}}^{s}=\sum\dot{\gamma}^{(k)}\,\mathbf{m}^{(k)}$ (1b) $\mathbf{m}^{(k)}=(\mathbf{n}^{(k)}\otimes\boldsymbol{\nu}^{(k)}+\boldsymbol{\nu}^{(k)}\otimes\mathbf{n}^{(k)})/2$

where $\mathbf{n}^{(k)}$, $\boldsymbol{\nu}^{(k)}$ are the unit slip plane normal and slip direction of kth slip systerm respectively, $\mathbf{m}^{(k)}$ is the Schmidt's orientation tensor of the systerm, $\dot{\gamma}^{(k)}$ slip shear rate of the systerm. Through volume averaging, total inelastic strain rate $\dot{\mathbf{E}}^{s}$ is written as:

(2) $\dot{\mathbf{E}}^{s}=\int\dot{\boldsymbol{\varepsilon}}^{s}\,dv/V$

For simplicity, we suppose that average number of active slip systerms is same and $\dot{\gamma}^{(k)}$ is also same as its average value $\dot{\gamma}^{(k)}$ in each grain or subgrain as did by Weng(1984), then we obtain:

(3a) $\dot{\mathbf{E}}^{s}=\sum\dot{\gamma}^{(k)}\,\mathbf{M}^{(k)}$ (3b) $\mathbf{M}^{(k)}=\int\mathbf{m}^{(k)}\,dv/V$

where $\mathbf{M}^{(k)}$ is the volume average of local Schmidt's orientation tensor $\mathbf{m}^{(k)}$.

Dislocation distributions in a polycrystalline,generally speaking, are diffent at different positions and directions, which depend upon the path of loading. Their directional feature can be described by directional distribution of orientation tensor $\mathbf{m}^{(k)}$.Natually this results in certain directional behavior of macroscopic inelastic strain rate and internal stresses such as the distortion of yield surfaces. Here, we will find out eigenvalues of macroscopic (average) orientation tensor $\mathbf{M}^{(k)}$ based on texture analysis (Bunge, 1982)

From the natures of local tensor $\mathbf{m}^{(k)}$

(4a) $tr\,(\mathbf{m}^{(k)})=0$ (4b) $tr\,(\mathbf{m}^{(k)})^{2}=0.5$ (4c) $tr\,(\mathbf{m}^{(k)})^{3}=0$

we can derive its three eigenvalues: $\lambda_1=0.5$, $\lambda_2=-0.5$, $\lambda_3=0$ (5)

Bunge(1982) had derived a general solution of symmetric second rank tensor for average quantity from local quantity with a arbitrary orientation distribution function. By means of this solution and (5), we obtain eigenvalues $E_1^{(k)}$, $E_2^{(k)}$, and $E_3^{(k)}$ of average tensor $\mathbf{M}^{(k)}$ as following:

(6a) $E_1^{(k)}=53(\,3\,C_2^{(k)}-C_1^{(k)})/30$, (6b) $E_2^{(k)}=-53(\,3C_2^{(k)}+C_1^{(k)})/30$

(6c) $E_3^{(k)}=53C_1^{(k)}/15$. From (6) we have:

(7) $f_k=\mathrm{tr}(M^{(k)})^2=53\sqrt{6}/30 * \sqrt{(C_1^{(k)})^2+(C_2^{(k)})^2}$

where texture coeffecients, obtained from directional distribution functions, $C_1^{(k)}$, $C_2^{(k)}$ are independent and characterize directional feature of dislocation distributions and may change with the path of loading and deformation history.

Following Aifantis(1987),we view a polycrystalline as a superposition of normal state (perfect lattice state) and a excited state (dislocation state) , and divide total applied stress into two parts: (8) $S=T^L+T^M$, $\mathrm{div}\, S=0$ where S is the total stress, T^L the lattice stress, T^M the dislocation stress. Then, inelastic work of macroscopic unit cell with volume V is written as:

(9a) $\dot{W}^z=T^L\dot{E}^z=T^L(\sum\dot{\gamma}^{(k)}M^{(k)})=\sum\dot{\gamma}^{(k)}\tau^{(k)}$, (9b) $\tau^{(k)}=T^LM^{(k)}=\int T^Lm^{(k)}dv/V$

Following Rice(1970), we assume that $\dot{\gamma}^{(k)}$ depends only on $\tau^{(k)}$, i.e. $\dot{\gamma}^{(k)}=G(\tau^{(k)})$, for example, for power-law creep: (10) $\dot{\gamma}^{(k)}=\dot{\gamma}_0^{(k)}|\tau^{(k)}/\tau_0|^m\, Sign(\tau^{(k)})$

For unified thermal activiated process, we derived the relation from absolute reaction-rate theory: (11) $\dot{\gamma}^{(k)}=\dot{\gamma}_0^{(k)}\sinh|\tau^{(k)}/\tau_0|^m\, \mathrm{sign}(\tau^{(k)})$

where we have supposed that the reference resolved shear stress is the same as τ_0 for each slip systerm, $\dot{\gamma}_0$ is the reference inelastic shear rate.

We choose active slip systerms based on maximum inelastic work principle (Bishop & Hill, 1951) which satisfies requirement of deformation compatibility and obtains a upper bound. The problem is the following maximization procedure (from (9), (10)):

(12) $\max \dot{W}^z=\max\sum\dot{\gamma}^{(k)}|\mathrm{tr}(T^LM^{(k)})|^{m+1}/(\tau_0)^m$, $\mathrm{tr}M^{(k)}=0$, $\mathrm{tr}(M^{(k)})^2=f_k^2$

The result is: (13) $M^{(k)}=f_kT/\sqrt{J_{2T}}\,\mathrm{sign}(\dot{\gamma}^{(k)})$, $\tau^{(k)}=f_k\sqrt{J_{2T}}\,\mathrm{sign}(\dot{\gamma}^{(k)})$

with (14) $T=T^L-\mathrm{tr}T^L/3$, $J_{2T}\equiv\mathrm{tr}(T)^2$

This result is general if $\dot{\gamma}^{(k)}$ obeys Rice's hypothesis. Using power-law series expansion of a function $G(\tau^{(k)})$, we can still derive (13)(14) in a similar manner. Combining (13), (3a), and (11), we obtain finally:

(15a) $\dot{E}^I=\sum f_k|\dot{\gamma}^{(k)}|T/\sqrt{J_{2T}}$, (15b) $|\dot{\gamma}^{(k)}|=\dot{\gamma}_0^{(k)}\sinh(f_k\sqrt{J_{2T}}/\tau_0)^m$

if directional distribution of dislocations is the same for each systerm, then, $f_k=f$, (15) is rewritten as: (16a) $\dot{E}^I=\dot{\gamma}_0\sinh(f\sqrt{J_{2T}}/\tau_0)^m f\, T/\sqrt{J_{2T}}$, $\dot{\gamma}_0=\sum\dot{\gamma}_0^{(k)}$

and (16b) $\dot{\xi}^I/f=\sum|\dot{\gamma}^{(k)}|\equiv\sqrt{\mathrm{tr}(\dot{E}^I)^2}$

4 EVOLUTION OF DISLOCATION STRESSES

It is reasonable to divide dislocation stress T^M (internal stress) into T^g and T^c corresponding to the processes of dislocation glide and climb respectively. T^g, glide internal stress which possesses the instantaneous behavior, characterizes the resistance of dislocation glide movements within the subgrains, and T^c, climb internal stress which forms gradually throughout the transient courses, characterizes the resistance of dislocation climb movements in the subgrain boundaries and in the interfaces near them. Therefore, we choose two kinds of time scale i.e. accumulated inelastic strain ξ^I and logarithmic Newton's time z to describe the glide and climb processes respectively. Furthermore we suppose internal stress T^g within subgrains and T^c in subgrain boundaries are all distributed uniformly. As average quantities (internal state variables) they also characterize the dislocation arrangement of substructures in a macroscopic way with the difinition:

(17a) $T^g=\sum T^{g(k)}$, $T^{g(k)}=2\alpha^{g(k)}Gb\sqrt{\rho^{g(k)}}M^{(k)}$ (17b) $T^c=2\alpha^cGb\sqrt{\rho^c}N$

where $\rho^{g(k)}$ is the average density of dislocations within subgrains of the kth systerm, ρ^c the average density of dislocations in subgrain boundaries. $\alpha^{g(k)}$, α^c, G, and b have common sense. N is defined by:

(18a) $N=\int n\, dv/V$ (18b) $n=(\mu\otimes\mu-I/3)$

where μ denotes unit normal of subgrain boundaries, I unit tensor. We approximately obtain time differential of internal stress under small strain condition:

(19a) $\dot{T}^{g(k)}\approx\alpha^{g(k)}Gb\dot{\rho}^{g(k)}M^{(k)}/\sqrt{\rho^{g(k)}}$ (19b) $\dot{T}^c\approx\alpha^cGb\,\dot{\rho}^cN/\sqrt{\rho^c}$

Following the point of view that the change of dislocation density is a competitive process between the storege of mobile dislocations and the recovery based on various mechanisms (Kocks, 1976), we derive the evolution equation of ρ^c as following:

(20) $d\rho^c/dz = A_c\sqrt{\rho^c}\ v^c - B_c\rho^c\sqrt{\rho^c}$ (21) $z=\log(1+t/t_0)$

where t_0 is a reference time. Average climb rate of dislocation $v^c \sim \sigma_e/\lambda$, and average climb distance λ may be assumed: $\lambda \sim d$, average size of subgrains $d \sim 1/\sigma_e$. Then, (20) is rewritten as:

(21) $d\rho^c/dz = A_c'(\sigma_e)^2\sqrt{\rho^c} - B_c\rho^c\sqrt{\rho^c}$ From (19b), (21) we obtain:

(22a) $dT^c/dz = [(E_s)^2(\sigma_e)^2 - (E_c)^2 J_{2c}]\ S'/\sqrt{J_{2s}}$

with (22b) $J_{2c} \equiv tr(T^c)^2$, $J_{2s} \equiv tr(S')^2$, $S' \equiv S - tr(S)/3$, $\sigma_e \equiv \sqrt{tr(S)^2}$

where Es,Ec are material constants. We also have assumed that the direction N of deformation resistance in subgrain boundaries identifies with S'.

Following Kocks(1976), the evolution of $\rho^{g(k)}$ is:

(23) $d\rho^{g(k)}/dt = \dot{\gamma}^{(k)}\sqrt{\rho^{g(k)}}/\beta b - L^{R(k)}\ \rho^{g(k)}(\sum|\dot{\gamma}^{(k)}|)/b$

where $L^{R(k)}$ is the swept-up length of disloction segement per recovery site.

We only conside weak coupling. i e. the effects of climb to glide for simplicity. Additional relaxation effects of glide internal stresses caused by the climb of dislocations through the interfaces in the manner of reaction-diffusion are mainly consided based on the experimental result (Orlova et al. 1973). These are taken into account through the increasing of $L^{R(k)}$ to $L^{R(k)\prime} = L^{R(k)}(1 + f_r(z))$ and interaction term $\rho^{g(k)}F(\rho^c)$.(23) is rewritten with the modifications as following:

(24) $d\rho^{g(k)}/dt = \dot{\gamma}^{(k)}\sqrt{\rho^{g(k)}}/\beta b - L^{R(k)\prime}\rho^{g(k)}\sum|\dot{\gamma}^{(k)}|/b - L^{R(k)\prime}\rho^{g(k)}F(\rho^c)$

From (3a), (24), (17) and (19a) we obtain:

(25a) $dT^g/dt = (\sum A^{(k)})\dot{E}^g - (\sum\alpha^{(k)}T^{g(k)})[\dot{\zeta}^I/f + F(\sqrt{J_{2c}}/B_0)]$

(25b) with $\alpha^{(k)} = \beta^{(k)}(1 + f_r(z))$, $f_r = A_{gc}(1 - \exp(-c_1 z))$, $F = \sinh(\sqrt{J_{2c}}/B_0)^{m}$

where $A^{(k)}$, $\beta^{(k)}$, A_{gc}, C_1, and B_0 are material contants.

Considering subgrain interiors as base material and subgrain boundaries as reinforced substructures that are k times higher than base in the strength against inelastic deformation, we derive following superposition rule of internal stress T^{gi} based on two phases model (Nix et al. 1980) as shown in fig.3

(26abc) $T^{gi} = T^g + f_x T^c$, $f_x = x/(1 + x)$, $x = k\ w/d$

where d is the average of subgrains,W the averege width of subgrain boundaries. The evolution of x is assumed as: (27) $dx/dz_1 = c_2(\sigma_e/c_3 - x)$ (28) $z_1 = \sigma_e z$

where c_2, c_3 are material constants.

5 VERIFICATION AND PREDICTION OF MODEL

We have finished the verification and prediction of the model proposed in this paper from systematic experimental results of bench mark problems for 2.25 Cr-1 Mo steel at 600℃ under uniaxial loading condition (Inoue et al. 1986, 1987). Using two curves of tension tests of constant strain rate 3.6/hr. and 0.36/hr. as well as steady values of creep tests of constant stresses, we have determined material constants as following (unit:stress: MPa; time: hr.; strain rate: 1/hr.; strain: mm/mm):

$\gamma_0 = 1.0$, $t_0 = 10^{-3}$, $m = 7.7$, $\tau_0 = 146.1$, $B_0 = 280.0$, $A_{gc} = 2.0$

$A^{(k)} = (82922.0,\ 12910.0,\ 1946.2)$; $\beta^{(k)} = 3.8333*(10^3,\ 10^2,\ 10^1)$

$E_s = 4.20*10^{-2}$, $E_c = 6.0*10^{-2}$, $c_1 = 0.4$, $c_3 = 120.6$, $c_2 = 2E_sE_c = 5.0*10^{-3}$

with $f_k = f = 1.0$

Comparision with experimental data have shown that the model can simulate and predict fairly accurately experimental results, specially for the mixed tests of creep-plasticity interaction, shown in fig.7 and fig.8. Another distinguishing feature of the model is that it successfully model both cases of plasticity and creep at the strain rate range from 10^{-6}/hr. to 10^1/hr. shown in fig.5 and fig. 6 and that it predicts the relaxation of glide internal stress due to the formation of dislocation substructures during transient creep and subsequent creep on the prior plastic deformation, shown in fig.6(b), fig.7(b)., which identifies with microscopic observation qualitatively (fig.1). An important result is that the saturated internal stress for creep is markedly larger than plasticity one and this difference increases with the increasing applied stress, as shown in fig.4.

REFERENCES

Ohashi, Y. etc. (1986). Effects of Prior Plasticity on Subsequent Creep of Type 316 Stainless Steel at Elevated Temperature, J.Eng.Mat.Tech., Vol.108,pp.68-74.

Fan, J. etc. (1989).Microscopically Based Constitutive Relations for Damage Mechanics & Creep-Plasticity Interaction.Nul. Eng. Des.Vol. 116,pp. 307-313

Contesti, E., Cailletaud,G.(1989). Description of Creep-Plasticity Interaction with Non-Unified Constitutive Equations. Nul. Eng. Des. Vol.116,pp. 330-336

Nix,W.D.,Ilscher,B.(1980). Mechanisms Controlling Creep of Single Phase Metals & Alloys, Strength of Metals & Alloys, Vol.3, pp.1503-1530, Pergamon Press.

Orlova,A., Cadek,J. (1973). Some Substructural Aspects of High-Temperature Creep in Metals. Phil. Mag., Vol.28, pp.891-899

Martin,J.L. (1985).Creep Behavior of Crystalline Solids,Swansea,Pineridge Press.

Frost, H.J., Ashby,M.F. (1982). Deformation Mechanism Maps, Oxford Press.

Rice,J.R. (1970).On the Structure of Stress Strain Relation for Time-Dependent Plastic Deformation in Metals, J. Appl. Mech., Sept., pp.728-737.

Aifantis, E. C. (1987) The Physics of Plastic Deformation. Int. J. Plasticity, Vol.3,p.211.

Kocks,U.F. (1976). Laws for Work-Hardening & Low-Temperature Creep, J. Eng.Mat. Tech. Vol.98, pp.76-85.

Inoue, T. etc. (1987). Evaluation of Inelastic Constitutive Models under creep Plasticity Interaction for 2.25 Cr-1 Mo Steel. Trans.SMiRT-9, Vol.L, pp.15-26

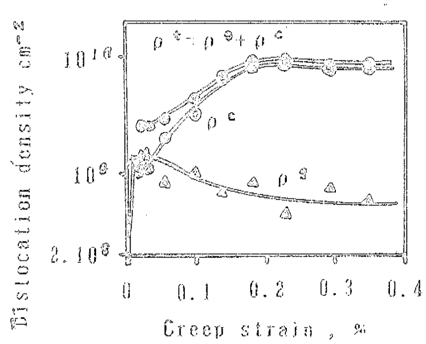

Fig.1 α-Fe single crystal creep

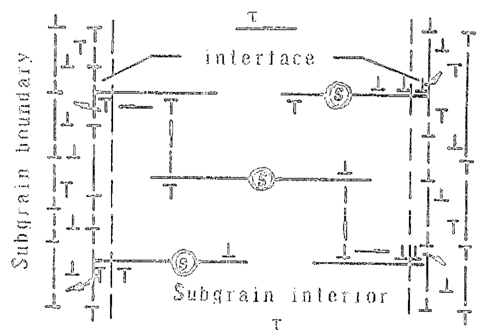

Fig.2 Schematic representation of glide-plus-climb mechanism

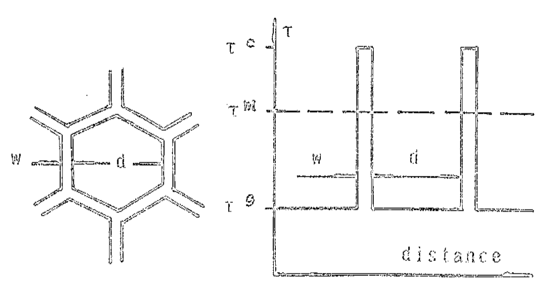

Fig.3 Two phases model and Superposition of internal stresses

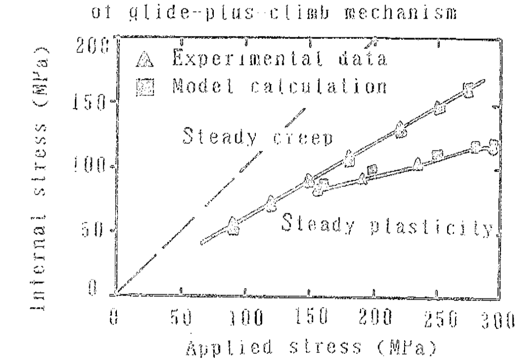

Fig.4 Relation between applied stress and saturated internal stress

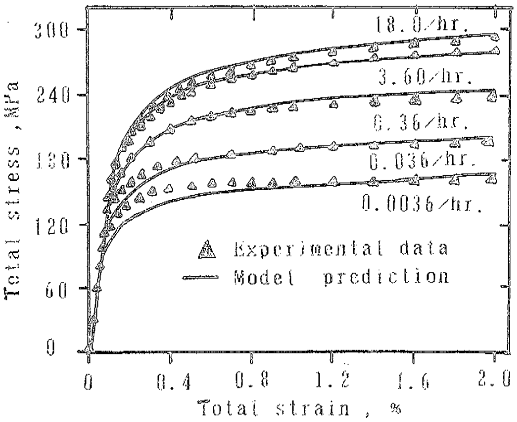

Fig.5 Tension at constant strain rates

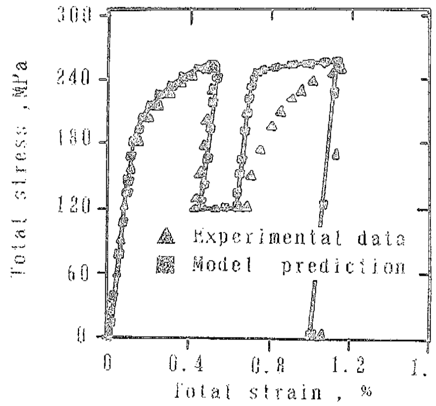

Fig.7(a) Plasticity-creep-plasticity

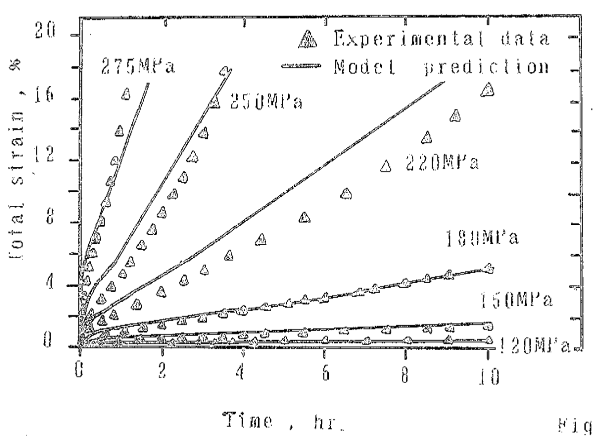

Fig.6(a) Creep at constant stress

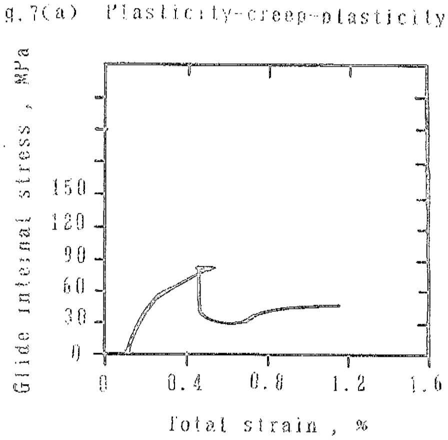

Fig.7(b) Relaxation of glide internal stress after plastic prestrain

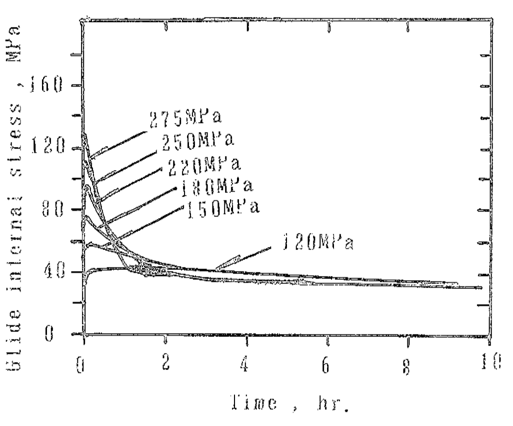

Fig.6(b) Relaxation of Glide internal stress during transient creep

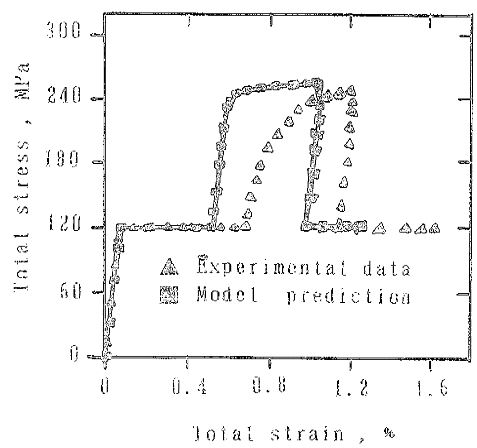

Fig.8 Creep-plasticity-creep